

Crystal Structure and Magnetic Properties of $\text{BaCu}_2(\text{PO}_4)_2$ Phosphate

A. MOQINE,* A. BOUKHARI,* AND J. DARRIET†

*Laboratoire de Chimie du Solide Appliquée, Département de Chimie, Faculté des Sciences, Université Mohammed V, B.P. 1014, Rabat, Morocco; and †Laboratoire de Chimie du Solide du CNRS 351, Cours de la libération, 33405 Talence Cedex, France

Received August 6, 1991; in revised form March 9, 1993; accepted March 17, 1993

The crystal structure of $\text{BaCu}_2(\text{PO}_4)_2$ has been determined from X-Ray single crystal data. The crystal symmetry is triclinic, space group $P\bar{1}$, with unit cell constants $a = 9.226(1) \text{ \AA}$, $b = 9.271(1) \text{ \AA}$, $c = 10.516(1) \text{ \AA}$, $\alpha = 106.76(5)^\circ$, $\beta = 101.69(5)^\circ$, and $\gamma = 115.70(5)^\circ$. The structure was solved using 2802 independent reflections ($R = 0.0411$, $R_w = 0.0413$). The framework corresponds to isolated sheets of mixed CuO_5 and PO_4 polyhedra which are linked by the Ba^{2+} cations. The copper atoms constitute isolated magnetic chains parallel to the [110] direction. The magnetic susceptibility of $\text{BaCu}_2(\text{PO}_4)_2$ has been interpreted in terms of a one-dimensional magnetic system. © 1993 Academic Press, Inc.

Introduction

The crystal structures of $AM_2(\text{PO}_4)_2$ phosphates, where $A = \text{Ca}, \text{Sr}$, or Ba and $M = \text{Mg}$ or divalent 3d cations, have been widely studied (1–11). $\text{CaZn}_2(\text{PO}_4)_2$ presents different allotropic forms: α , β , γ , and δ (1). The transition temperatures are respectively 870°C, 997°C, and 1013°C. The γ form is stabilized by a fast quench at 1013°C. The crystal structure of the α form (triclinic symmetry) has been recently determined for a single crystal (4). The β forms of $\text{CaZn}_2(\text{PO}_4)_2$ and $\text{BaZn}_2(\text{PO}_4)_2$ are isostructural with the silicate $\text{BaAl}_2(\text{SiO}_4)_3$ (3) (7). Two allotropic forms of $\text{SrZn}_2(\text{PO}_4)_2$ have been isolated, with a phase transition temperature of 1305° (2). The low temperature form is monoclinic (5). $\text{BaMg}_2(\text{PO}_4)_2$ also shows two reversible phase transitions at 820°C (6).

The $\text{BaM}_2(\text{PO}_4)_2$ ($M = \text{Ni}, \text{Co}$) phosphates and their homologous arseniates are isostructural. Their crystal symmetry is rhombohedral (space group $R\bar{3}$) (7–9). In the case of $\text{BaCo}_2(\text{PO}_4)_2$ a high temperature form, isostructural with $\text{BaZn}_2(\text{PO}_4)_2$, has been reported (10). The two-dimensional

magnetic properties of $\text{BaM}_2(\text{PO}_4)_2$ ($M = \text{Co}, \text{Ni}$) have been widely studied (11–15). This paper deals with the crystal structure and magnetic properties of the new phosphate $\text{BaCu}_2(\text{PO}_4)_2$.

Experimental

$\text{BaCu}_2(\text{PO}_4)_2$ has been prepared by heating a mixture of $(\text{NH}_4)_2\text{HPO}_4$, BaCO_3 , and CuO in the molar ratio 2 : 1 : 2. The reaction is carried out in a platinum crucible. The mixture, after being ground, is slowly heated to 1000°C and cooled to 800°C with a cooling rate of 5°C/h. Then the product is furnace cooled down to room temperature. By this procedure single crystals of $\text{BaCu}_2(\text{PO}_4)_2$ have been isolated.

Preliminary photographic studies show that the symmetry is triclinic. Using Ge as a standard, the X-ray diffraction pattern of $\text{BaCu}_2(\text{PO}_4)_2$ can be indexed with the cell parameters $a = 9.226(1) \text{ \AA}$, $b = 9.271(1) \text{ \AA}$, $c = 10.516(1) \text{ \AA}$, $\alpha = 106.76(5)^\circ$, $\beta = 101.69(5)^\circ$, and $\gamma = 115.70(5)^\circ$. In fact very weak reflections have been observed on photographic films which can be indexed in

TABLE I
CRYSTAL DATA AND CONDITIONS OF DATA COLLECTION AND REFINEMENT
FOR BaCu₂(PO₄)₂

Symmetry: Triclinic	Space group: $P\bar{1}$		
Cell dimensions:	$a = 9.226(1)$ Å	$b = 9.271(1)$ Å	$c = 10.516(1)$ Å
	$\alpha = 106.76(5)^\circ$	$\beta = 101.69(5)^\circ$	$\gamma = 115.70(5)^\circ$
	$V = 717.96$ Å ³	$Z = 4$	$d_{\text{cal}} = 4.20 \text{ g} \cdot \text{cm}^{-3}$
Radiation: MoK _α (graphite monochromatized)			
Range measured: $1^\circ < \theta < 30^\circ$	h, k, l min/max:	-16, +16	
Angle for ω -scan (°): $2 + 3 \tan \theta$			
Number of measured reflections: 6812; independent: 2802 with $I > 3\sigma(I)$			
Absorption correction: empirical from Psi-scan ($\mu(\text{MoK}_\alpha) = 114.08 \text{ cm}^{-1}$)			
Extinction ϵ refined in F_c (corr.) = $F_c(1 - \epsilon F_c^2 / \sin \theta)$	$\epsilon = 2.9 \times 10^{-7}$		
$R = \sum D / \sum F_o $: 0.0411		
$wR = (\sum \omega D^2 / \sum \omega F_o^2)^{1/2}$: 0.0413		
with $D = \sum F_o - F_c $ and weights ω proportional to $1/\sigma^2(F_o)$.			

a super cell corresponding to a pseudo-monoclinic symmetry (*C*-centered) which is four times larger than the elementary cell. The relationships between the two cells are $\mathbf{a}_2 = (\mathbf{a}_1 + \mathbf{b}_1)/2$, $\mathbf{b}_2 = (\mathbf{a}_1 - \mathbf{b}_1)/2$, and $\mathbf{c}_2 = -(\mathbf{c}_1 + \mathbf{a}_1)/2$. The subscripts 1 and 2 correspond respectively to the elementary triclinic cell and to the pseudomonoclinic one. These weak reflections are too small in number to be considered in the crystal structure determination.

The single crystal selected for X-ray data collection was mounted on a four circles automatic diffractometer CAD4 (Enraf-Nonius) and data were collected using graphite-monochromated MoK_α radiation. The conditions are listed in Table I. The intensities, corrected for Lorentz-polarization effects as well as for absorption, using empirical absorption corrections in the SDP program, were averaged and gave an R_{av} value of 0.020. The scattering factors were taken from (16) and the influence of anomalous dispersion (17) was included. The structure refinement was performed using the SHELX program (18).

The structure was solved from the Patterson map and the barium atoms were first located. From successive difference Fourier maps and refinements, the remaining atoms were located and the final R values decreased to $R = 0.0411$ ($R_w = 0.0413$). The final positional and thermal parameters

are reported in Tables II and III. A table specifying the calculated and observed structure factors can be obtained on request to the authors.

TABLE II
FRACTIONAL COORDINATES AND EQUIVALENT ISOTROPIC TEMPERATURE FACTORS B_{eq} (Å²) FOR BaCu₂(PO₄)₂

Atom	x	y	z	B_{eq} (Å ²)
Ba(1)	0.2417(1)	0.2446(1)	-0.0023(1)	0.96(1)
Ba(2)	0.2635(1)	0.2485(1)	0.4868(1)	1.05(1)
Cu(1)	0.4828(1)	0.8288(1)	0.1956(1)	0.74(2)
Cu(2)	0.0303(1)	0.6897(2)	0.8006(1)	0.94(2)
Cu(3)	0.3660(1)	0.7103(1)	0.6897(1)	0.62(2)
Cu(4)	0.0991(2)	0.7642(2)	0.2939(1)	1.15(2)
P(1)	0.1956(3)	0.9205(3)	0.6287(2)	0.52(3)
P(2)	0.2127(3)	0.9436(3)	0.1351(2)	0.56(3)
P(3)	0.2965(3)	0.5763(3)	0.3591(2)	0.57(3)
P(4)	0.2882(3)	0.5692(3)	0.8662(2)	0.56(3)
O(1)	0.2731(8)	0.1094(9)	0.7426(7)	1.18(5)
O(2)	0.0444(8)	0.7815(10)	0.6421(8)	1.52(5)
O(3)	0.1363(9)	0.9200(8)	0.4829(6)	1.06(5)
O(4)	0.3573(7)	0.8986(8)	0.6566(7)	0.78(5)
O(5)	0.2629(7)	0.8091(8)	0.1497(6)	0.76(5)
O(6)	0.1050(9)	0.9450(10)	0.2295(7)	1.41(5)
O(7)	0.3621(8)	0.1267(9)	0.1822(9)	2.22(5)
O(8)	0.0913(8)	0.8797(8)	0.9801(6)	0.81(5)
O(9)	0.3752(9)	0.5908(9)	0.5074(6)	1.00(5)
O(10)	0.1361(8)	0.5942(8)	0.3417(6)	0.87(5)
O(11)	0.2143(8)	0.3818(9)	0.2522(7)	1.21(5)
O(12)	0.4389(9)	0.7036(11)	0.3322(9)	1.89(5)
O(13)	0.4364(8)	0.6524(9)	0.0107(6)	0.94(5)
O(14)	0.2523(8)	0.7117(9)	0.8388(6)	0.78(5)
O(15)	0.3511(9)	0.5185(8)	0.7447(7)	1.06(5)
O(16)	0.1335(9)	0.4186(10)	0.8654(7)	1.47(5)

TABLE III
ANISOTROPIC TEMPERATURE FACTORS^a $U_{ij} \times 10^4$ FOR $\text{BaCu}_2(\text{PO}_4)_2$

Atom	U_{11}	U_{22}	U_{33}	U_{12}	U_{13}	U_{23}
Ba1	106(2)	224(3)	139(2)	132(2)	79(2)	121(2)
Ba2	103(2)	57(2)	165(3)	16(2)	-36(2)	42(2)
Cu1	67(4)	112(5)	85(4)	18(4)	4(3)	58(4)
Cu2	80(4)	151(5)	90(4)	-8(4)	-2(3)	85(4)
Cu3	118(4)	73(4)	67(4)	36(3)	28(3)	68(4)
Cu4	257(6)	116(5)	74(4)	28(4)	7(4)	139(5)
P1	52(8)	64(9)	56(8)	26(7)	0(6)	20(7)
P2	68(8)	57(9)	78(8)	29(7)	7(7)	33(7)
P3	58(8)	71(9)	67(8)	31(7)	6(7)	24(7)
P4	62(8)	83(9)	52(8)	28(7)	3(7)	35(8)
O1	101(25)	163(30)	89(25)	-48(22)	-19(20)	83(24)
O2	56(25)	241(36)	250(34)	176(29)	25(24)	25(26)
O3	279(32)	145(28)	29(23)	31(21)	47(22)	160(26)
O4	48(23)	75(26)	181(28)	70(22)	47(21)	26(21)
O5	55(23)	84(26)	136(27)	34(22)	17(20)	41(21)
O6	241(33)	250(36)	175(30)	121(27)	117(26)	196(31)
O7	74(26)	179(32)	421(42)	213(30)	-126(26)	-25(23)
O8	136(27)	146(28)	75(23)	55(20)	29(20)	111(25)
O9	208(31)	204(33)	95(26)	97(24)	76(23)	178(29)
O10	125(25)	151(28)	161(27)	108(22)	62(21)	128(23)
O11	117(27)	126(30)	119(27)	-57(22)	-6(12)	77(25)
O12	101(28)	308(43)	297(41)	237(37)	38(27)	46(29)
O13	121(26)	190(32)	51(23)	24(21)	-8(20)	120(26)
O14	94(25)	145(29)	120(26)	89(23)	52(21)	88(24)
O15	245(33)	112(28)	121(27)	72(23)	105(26)	124(27)
O16	150(29)	196(34)	181(30)	142(27)	6(24)	52(27)

^a The vibrational coefficients relate to the expression $T = \exp[-2\pi^2(h^2a^{*2}U_{11} + h^2b^{*2}U_{22} + l^2c^{*2}U_{33} + 2hka^{*}b^{*}U_{12} + 2hla^{*}c^{*}U_{13} + 2klb^{*}c^{*}U_{23})]$.

Description of the Structure

The structure of the $\text{BaCu}_2(\text{PO}_4)_2$ projected onto the (001) plane is given in Fig. 1. The framework is formed by parallel

$[\text{CuPO}_4]_n^{n-}$ sheets linked together by the Ba^{2+} cations. The main interatomic distances and angles are given in Table IV.

The copper atoms occupy four independent crystallographic sites and the surrounding oxygens constitute deformed trigonal pyramids in each case. This type of environment for Cu^{2+} is similar to those observed previously in $\text{Cu}_3(\text{PO}_4)_2$ and $\text{Ca}_3\text{Cu}_3(\text{PO}_4)_4$ (19, 20).

The mean Cu-O bond distances in the equatorial plane for Cu(1), Cu(2), Cu(3), and Cu(4) are respectively 2.062, 2.072, 2.050, and 2.101 Å and longer than the axial distances (1.937 (Cu(1)), 1.934 (Cu(2)), 1.945 (Cu(3)), and 1.946 Å (Cu(4))). The angle values between the axial Cu-O bonds vary from 170.8° for Cu(1) to 166.8° for Cu(4) (Table IV).

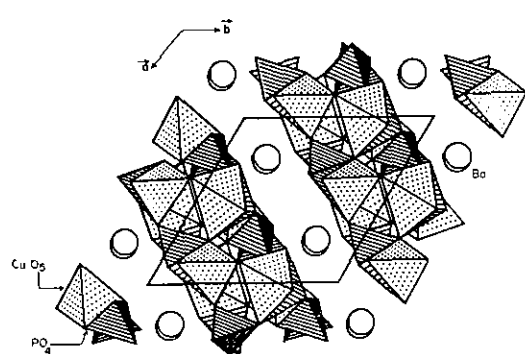


FIG. 1. Projection of the structure of $\text{BaCu}_2(\text{PO}_4)_2$ on (001).

TABLE IV
INTERATOMIC DISTANCES (Å) AND ANGLES (°) IN BaCu₂(PO₄)₂

Polyhedron Ba(1)O ₈				Polyhedron Ba(2)O ₈			
Ba(1)–O(11)	2.726(6)	Ba(1)–O(16)	2.768(7)	Ba(2)–O(3)	2.732(7)	Ba(2)–O(6)	2.796(7)
–O(13')	2.727(7)	–O(8')	2.862(7)	–O(2')	2.743(7)	–O(9)	2.803(7)
–O(1)	2.747(6)	–O(6')	2.938(7)	–O(12')	2.774(7)	–O(9')	2.981(7)
–O(7)	2.755(7)	–O(8)	2.977(7)	–O(15)	2.778(6)	–O(11)	3.100(7)
$\langle \text{Ba}(1)–\text{O} \rangle = 2.813$				$\langle \text{Ba}(2)–\text{O} \rangle = 2.838$			
Polyhedron Cu(1)O ₅	Polyhedron Cu(2)O ₅		Polyhedron Cu(3)O ₅	Polyhedron Cu(4)O ₅			
Cu(1)–O(5)	1.900(5)	Cu(2)–O(14)	1.912(5)	Cu(3)–O(4)	1.906(6)	Cu(4)–O(10)	1.925(6)
–O(13)	1.965(7)	–O(8)	1.943(5)	–O(9)	1.958(6)	–O(3)	1.947(5)
–O(1')	1.974(7)	–O(11')	1.955	–O(15)	1.983(6)	–O(6)	1.966(7)
–O(12)	2.088(7)	–O(2)	2.079(5)	–O(14)	2.056(6)	–O(16')	2.009(5)
–O(4')	2.134(7)	–O(10')	2.195(5)	–O(7')	2.136(6)	–O(5)	2.346(6)
$\langle \text{Cu}(1)–\text{O} \rangle = 2.012$	$\langle \text{Cu}(2)–\text{O} \rangle = 2.017$		$\langle \text{Cu}(3)–\text{O} \rangle = 2.008$	$\langle \text{Cu}(4)–\text{O} \rangle = 2.039$			
O5–Cu1–O13	97.7(3)	O14–Cu2–O8	97.6(3)	O4–Cu3–O9	98.4(3)	O10–Cu4–O3	99.5(3)
–O1'	170.8(3)	–O11'	168.9(3)	–O15	170.0(2)	–O6	166.8(3)
–O12	93.6(3)	–O2	94.6(3)	–O14	97.1(2)	–O16'	94.0(3)
–O4'	100.0(3)	–O10'	99.9(3)	–O7'	92.2(3)	–O5	99.3(3)
O13–Cu1–O1'	89.0(3)	O8–Cu2–O11'	91.2(3)	O9–Cu3–O15	90.2(3)	O3–Cu4–O6	87.6(3)
–O12	107.5(3)	–O2	109.6(3)	–O14	151.6(3)	–O16'	125.7(3)
–O4'	144.3(3)	–O10'	146.7(3)	–O7'	99.6(3)	–O5	131.2(3)
O1'–Cu1–O12	90.8(3)	O11'–Cu2–O2	90.2(3)	O15–Cu3–O14	73.0(2)	O6–Cu4–O16'	90.9(3)
–O4'	71.0(3)	–O10'	69.3(3)	–O7'	91.3(3)	–O5	67.9(2)
O12–Cu1–O4'	102.4(3)	O2–Cu2–O10'	97.8(3)	O14–Cu3–O7'	103.6(3)	O16'–Cu4–O6	97.6(3)
Tetrahedron P(1)O ₄	Tetrahedron P(2)O ₄		Tetrahedron P(3)O ₄	Tetrahedron P(4)O ₄			
P(1)–O(2)	1.501(7)	P(2)–O(7)	1.496(7)	P(3)–O(12)	1.483(7)	P(4)–O(16)	1.499(7)
–O(3)	1.518(6)	–O(5)	1.541(6)	–O(9)	1.521(6)	–O(13)	1.530(6)
–O(1)	1.539(6)	–O(6)	1.541(7)	–O(10)	1.539(6)	–O(15)	1.543(7)
–O(4)	1.573(6)	–O(8)	1.546(6)	–O(11)	1.547(7)	–O(14)	1.580(6)
$\langle \text{P}(1)–\text{O} \rangle = 1.533$	$\langle \text{P}(2)–\text{O} \rangle = 1.531$		$\langle \text{P}(3)–\text{O} \rangle = 1.523$	$\langle \text{P}(4)–\text{O} \rangle = 1.538$			
O(2)–P(1)–O(3)	109.1(4)	O(7)–P(2)–O(5)	115.3(4)	O(12)–P(3)–O(9)	107.3(4)	O(16)–P(4)–O(13)	107.2(4)
–O(1)	113.9(4)	–O(6)	110.2(5)	–O(10)	115.8(4)	–O(15)	115.8(4)
–O(4)	112.6(4)	–O(8)	108.3(4)	–O(11)	113.1(5)	–O(14)	113.6(4)
O(3)–P(1)–O(1)	107.2(4)	O(5)–P(2)–O(6)	103.9(4)	O(9)–P(3)–O(10)	112.0(3)	O(13)–P(4)–O(15)	108.8(4)
–O(4)	112.2(3)	–O(8)	111.9(3)	–O(11)	106.6(4)	–O(14)	111.3(4)
O(1)–P(1)–O(4)	101.7(4)	O(6)–P(2)–O(8)	106.8(3)	O(10)–P(3)–O(11)	101.7(3)	O(15)–P(4)–O(14)	100.7(3)

Note. Symmetry code: $i = x \ y \ z$; $i' = \bar{x} \ \bar{y} \ \bar{z}$.

The P–O bond distances range between 1.523 and 1.538 Å and are in good agreement with those generally observed in other phosphates.

In each layer the CuO₅ bipyramids and the PO₄ tetrahedra are linked by edge and corner sharing. One CuO₅ polyhedron is linked to four (PO₄) tetrahedra by corner sharing and by edge sharing to one tetrahedra.

The main feature of the structure is that the CuO₅ bipyramids constitute isolated magnetic chains in which the bipyramids share corners as it is represented in Fig. 2. In each [CuPO₄]_n⁺ layer these magnetic chains are isolated by the (PO₄) tetrahedra and between the sheets by the Ba²⁺ cations.

The Ba²⁺ cations (Ba(1) and Ba(2)) are linked to eight oxygen atoms. The Ba(1)–O bond distances vary between 2.726 and

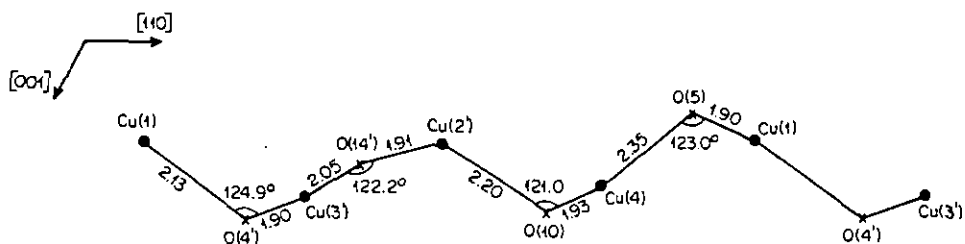


FIG. 2. Bridged oxygen ions with Cu–O–Cu angles ($^{\circ}$) and Cu–O bond distances (\AA) along the copper chain in $\text{BaCu}_2(\text{PO}_4)_2$.

2.977 \AA and the Ba(2)–O distances between 2.736 and 3.100 \AA . These values are similar to those observed in $\text{Ba}_3(\text{PO}_4)_2$, for example (21).

Magnetic Properties

The magnetic susceptibility of $\text{BaCu}_2(\text{PO}_4)_2$ has been determined for a powder sample using a SQUID magnetometer (S.H.E. Corp.) in the temperature range, $4.2 < T < 300 \text{ K}$ (Fig. 3). The large maximum observed around 65 K is characteristic of a one-dimensional, low dimensionality antiferromagnetic magnetic system. The minimum observed at 10 K can be explained by the fact that the measurements are made on powder samples for which the length of the chains is finite, and also by small amounts of paramagnetic impurity. As mentioned above, the Cu^{2+} cations constitute isolated magnetic chains with four types of intrachain distances. Until now there has been no Heisenberg model for this type of magnetic

chain in which four types of exchange interactions are considered. The only case developed in the literature is that of two alternating interactions, J and αJ (22, 23). The Heisenberg Hamiltonian is $H_{\text{exch}} = -2J \sum_{i=1}^{N/2} (S_{2i}S_{2i-1} + \alpha S_{2i}S_{2i+1})$.

The mathematical form of the magnetic susceptibility for $S = \frac{1}{2}$ has been solved in Ref. (23) and was applied to our case. The best fit is obtained for $J/k = -51.6 \text{ K}$ and $\alpha = 0.96$ with $g = 2.06$ (see Fig. 3). As can be seen in Fig. 3, the agreement between the observed and calculated magnetic susceptibility is not very accurate. This may be because only two types of exchange interactions are considered, whereas there are four types of J values associated with the four Cu–Cu intrachain distances.

In conclusion, the crystal structure of $\text{BaCu}_2(\text{PO}_4)_2$ has been determined for a single crystal. It is a new member in the series of $AM_2(\text{PO}_4)_2$ phosphates in which A represents Ca, Sr, or Ba and $M = \text{Mg}$ or a divalent 3d transition metal.

The copper atoms are located in deformed trigonal bipyramids and constitute isolated magnetic chains. These results have been confirmed by magnetic measurements. The magnetic susceptibility shows a large maximum around $T = 65 \text{ K}$, which is characteristic of antiferromagnetic one-dimensional magnetic systems.

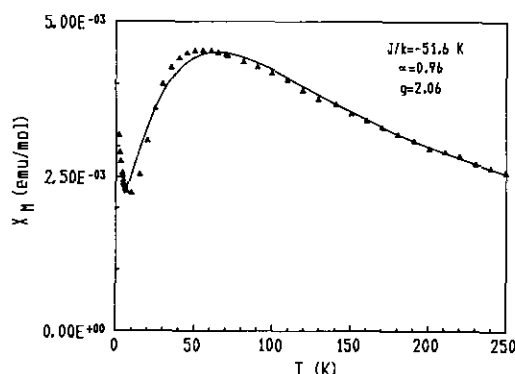


FIG. 3. Calculated (—) and experimental (Δ) data of the magnetic susceptibility of $\text{BaCu}_2(\text{PO}_4)_2$.

References

1. J. F. SARVER, M. V. HOFFMAN, AND F. A. HUMMEL, *J. Electrochem. Soc.* **108**, 1103 (1961).
2. E. R. KREIDLER AND F. A. HUMMEL, *Inorg. Chem.* **6** (3), 524 (1967).

3. C. A. SORREL, *Am. Mineral.* **47**, 291 (1962).
4. R. J. B. JAKEMAN AND A. K. CHEETHAM, *J. Am. Chem. Soc.* **110** (4), 1140 (1988).
5. A. HEMON AND G. COURBION, *J. Solid State Chem.* **85**, 164 (1990).
6. M. V. HOFFMAN, *J. Electrochem. Soc.* **110**, 1223 (1963).
7. S. EYMOND, Thèse de 3^{ème} cycle, Grenoble (1968).
8. S. EYMOND, C. MARTIN, AND A. DURIF, *Mater. Res. Bull.* **4**, 595 (1960).
9. L. P. REGNAULT, Thèse de 3^{ème} cycle, Grenoble (1976).
10. J. Y. HENRY, Thèse d'état, Grenoble (1976).
11. L. P. REGNAULT, P. BURLET, AND J. R. MIGNOD, *Physica* **86-88B**, 660 (1977).
12. L. P. REGNAULT, J. R. MIGNOD, J. VILLAIN, AND A. DE COMBRIEU, *J. Phys.* **39** (8), C6-759 (1978).
13. L. P. REGNAULT, J. Y. HENRY, J. R. MIGNOD, AND L. J. DE JONGH, *J. Magn. Magn. Mater.* **15-18**, 1021 (1980).
14. L. P. REGNAULT, J. R. MIGNOD, AND A. DE COMBRIEU, *J. Magn. Magn. Mater.* **31-34**, 1205 (1983).
15. L. P. REGNAULT, J. P. BOUCHER, J. R. MIGNOD, J. BOUILLOT, R. PYNN, J. Y. HENRY, AND J. R. RENARD, *Physica* **136B**, 329 (1986).
16. D. T. CROMER AND J. D. MANN, *Acta Crystallogr. Sect. A* **24**, 321 (1968).
17. D. T. CROMER AND D. LIBERMAN, *J. Chem. Phys.* **53**, 1891 (1970).
18. G. SHELDICK, "SHELX 76 Program for Crystal Structure Determination," Cambridge Univ. Press, London/New York (1976).
19. G. L. SHOEMAKER, J. B. ANDERSON, AND E. KOSTINER, *Acta Crystallogr. Sect. B* **33**, 2969 (1977).
20. J. B. ANDERSON, E. KOSTINER, AND A. RUSZALA, *J. Solid State Chem.* **39**, 29 (1981).
21. W. H. ZACHARIAZEN, *Acta Crystallogr.* **1**, 263 (1948).
22. W. DUFFY AND K. P. BARR, *Phys. Rev.* **165**, 647 (1968).
23. W. E. HATFIELD, *J. Appl. Phys.* **52**, 1985 (1981).